



ELSEVIER

# Nitrogen effects on the microstructural evolution of carbon films under thermal annealing

N. Laidani<sup>a,\*</sup>, L. Guzman<sup>a</sup>, A. Miotello<sup>b</sup>, R.S. Brusa<sup>b</sup>, G.P. Karwasz<sup>b</sup>, A. Zecca<sup>b</sup>,  
C. Bottani<sup>c</sup>, J. Perrière<sup>d</sup>

<sup>a</sup> Centro Materiali e Biofisica Medica, 38050 Povo, Trento, Italy

<sup>b</sup> Dipartimento di Fisica, Università di Trento, 38050 Povo, Trento, Italy

<sup>c</sup> Dipartimento di Ingegneria Nucleare, Politecnico di Milano, via Ponzo 34/3, 20133 Milano, Italy

<sup>d</sup> Groupe de Physique des Solides, CNRS, Université de Paris VII-VI, 2, Place Jussieu, Tour 23, 75251 Paris, France

## Abstract

Nitrogenated C-films (CN<sub>x</sub>) were prepared either by rf reactive sputtering of graphite or by N<sup>+</sup>-implantation with energies of 30–90 keV. The structural evolution of these films under thermal vacuum annealing, at various temperatures was investigated by means of Raman analysis and positron annihilation spectroscopy (PAS). The atomic film composition was determined by Nuclear Reaction Analysis (NRA) and Elastic Recoil Detection (ERD). Nitrogen incorporation in the C films increases their amorphicity and its effect on the void concentration is connected to the nature of the nitrogenation process. Upon thermal annealing, the CN<sub>x</sub> film structure degrades more rapidly than do the C films, increasing the disordered graphitic phase content. The structural changes of the C and the CN<sub>x</sub> films are associated with H and N dynamical behaviour induced by annealing.

## 1. Introduction

The vapor-phase growth and the characterization of nitrogenated carbon films (CN<sub>x</sub>) have generated an increasing interest in recent years. For the synthesis of such films, various techniques have been applied: reactive sputtering of graphite [1], plasma decomposition of N<sub>2</sub> mixed with various hydrocarbon [2], ion beam assisted deposition [3] and ion-implantation [4]. Although considerable attention has been devoted to understand the microstructure of the CN<sub>x</sub> films, we are not aware of a study of the evolution of the microstructure of such films under post-deposition annealing treatments.

In a previous work, we studied the mechanical properties and the chemical and electronic structure of CN<sub>x</sub> films produced by N<sup>+</sup>-implantation in C-films and by reactive sputtering of graphite [5,6]. The C-films have been found to retain their starting diamond-like character after the N-incorporation and showed an improved friction behaviour. In this work, we report the nitrogen effects on the microstructural behaviour of C-films under thermal annealing. We had characterized these films with Raman and positron annihilation spectroscopies. Nuclear reaction

(NRA) and elastic recoil detection (ERD) provided information about the elemental composition of the films.

## 2. Experimental

The C-films were sputter deposited on silicon substrates, from a graphite target in a rf planar magnetron discharge at 1 Pa and 100 W. Details of the deposition parameters can be found in [5]. The N-doped C-films were prepared in two different ways: (1) by N<sup>+</sup>-implantation of the C-films (ii-CN<sub>x</sub> films) or (2) by reactive sputtering of a graphite target in a 50% Ar–50% N<sub>2</sub> discharge (rs-CN<sub>x</sub> films), carried out in the same conditions as for the C-film deposition. Thickness measurements were performed by means of a DEKTAK IIA profilometer and the mass measurements with a Mettler H51AR balance. N<sup>+</sup>-implantation in C-films, took place at normal incidence, at room temperature with a current density of about 5 μA/cm<sup>2</sup> and at a fluence of 2 × 10<sup>17</sup> ions/cm<sup>2</sup>. Two ion energies were used: 30 keV for 100 nm thick films, (the projected ion range is R<sub>p</sub> = 76 nm) and 90 keV for 400 nm thick films (R<sub>p</sub> = 210 nm). The ion range has been computed by means of the TRIM'95 numerical code [7]. The thermal annealings were performed by heating, under vacuum (10<sup>-6</sup> Pa), the samples from room temperature to 773 K or 1073 K at 10°C/min. The atomic composition of the films

\* Corresponding author. Fax: +39-461-881696; email: Laidani@alpha.science.unitn. it.

was determined by NRA and ERD. Absolute amounts of C, N and O were obtained through the  $^{12}\text{C}(\text{d,p})$   $^{13}\text{C}$ ,  $^{14}\text{N}(\text{d,p})$   $^{15}\text{N}$  and  $^{16}\text{O}(\text{d,p})$   $^{17}\text{O}$  reactions. ERD was used to determine the absolute H content in the films. In this case, the samples were bombarded by 1.9 MeV  $\alpha$  particles at an incidence angle of  $15^\circ$ , while the detection angle was set at  $30^\circ$ . The hydrogen concentrations have been extracted from the experimental data by the SENRAS simulation program [8]. Room temperature Raman spectra of the films were recorded in a Jobin Yvon T64000 apparatus, using an  $\text{Ar}^+$  ion laser as a light source operating at 514.5 nm. The positron annihilation spectroscopy (PAS) measurements were done with a low energy positron beam tuneable from 0.2 to 30 keV that permitted to investigate the sample from the surface to some microns in depth. The positron trapping by defects was detected by the Doppler broadening technique.

### 3. Results and discussion

#### 3.1. Atomic composition and density

##### 3.1.1. As-prepared films

The experimental results on atomic composition and density, obtained with NRA and ERD, for a C-film and a 30 keV  $\text{N}^+$ -implanted carbon film, both 100 nm thick, are presented in Table 1. The N/C atomic ratio and the mass density of the C, ii-CN<sub>x</sub> and rs-CN<sub>x</sub> films are displayed in Table 2. The  $2 \times 10^{17}$  N/cm<sup>2</sup> dose yields a global N/C atomic ratio of 0.24 in the ii-CN<sub>x</sub> film. The mass density value of the C-film,  $(1.73 \pm 0.34)$  g/cm<sup>3</sup>, is typical of amorphous films [9,10]. It is higher in the ii-CN<sub>x</sub> film. A compositional depth profile obtained for the rs-CN<sub>x</sub> films

Table 1  
Atomic composition of the C-films and ii-CN<sub>x</sub> films before and after annealing at 773 K and 1073 K

Atomic composition (atom/cm <sup>2</sup> )	Films	
	C	ii-CN <sub>x</sub>
	before annealing	
C ( $\pm 10\%$ )	$824 \times 10^{15}$	$807 \times 10^{15}$
H ( $\pm 5\%$ )	$205 \times 10^{15}$	$250 \times 10^{15}$
O ( $\pm 3\%$ )	$40 \times 10^{15}$	$57 \times 10^{15}$
N ( $\pm 5\%$ )	–	$192 \times 10^{15}$
	after annealing at 773 K	
C ( $\pm 10\%$ )	$675 \times 10^{15}$	$825 \times 10^{15}$
H ( $\pm 5\%$ )	$145 \times 10^{15}$	$140 \times 10^{15}$
O ( $\pm 3\%$ )	$37 \times 10^{15}$	$56 \times 10^{15}$
N ( $\pm 5\%$ )	–	$142 \times 10^{15}$
	after annealing at 1073 K	
C ( $\pm 10\%$ )	$692 \times 10^{15}$	$804 \times 10^{15}$
H ( $\pm 5\%$ )	$54 \times 10^{15}$	$51 \times 10^{15}$
O ( $\pm 3\%$ )	$55 \times 10^{15}$	$44 \times 10^{15}$
N ( $\pm 5\%$ )	–	$13 \times 10^{15}$

Table 2  
N/C atomic ratio and mass density of the C, ii-CN<sub>x</sub> and rs-CN<sub>x</sub> films

Films	C	ii-CN <sub>x</sub>	rs-CN <sub>x</sub>
N/C	–	0.24	0.07
Mass density (g/cm <sup>3</sup> )	$1.73 (\pm 20\%)$	$2.20 (\pm 20\%)$	$2.61 (\pm 10\%)$

by Auger electron spectroscopy (plot not shown) gave a N content almost constant within the film and of 7 at.%. The atomic density, as obtained by mass measurements, was  $(2.61 \pm 0.26)$  g/cm<sup>3</sup>.

Although not intentionally added, the samples contained hydrogen which came from gas phase contamination, as did oxygen, also present. For the latter, we do not exclude also a post-deposition contamination. The values reported in Table 1 for H content include the H content both in the film and the substrate. In Fig. 1a and b are reported the ERD H concentration profiles, as a function of depth, in C and ii-CN<sub>x</sub> films respectively. In the unimplanted specimen, the hydrogen profile is flat and extends down into the substrate. The actual H/C ratio in the C-films is 0.14, a value below the usual hydrogen concentration range in hydrogenated C films [11]. The ii-CN<sub>x</sub> film exhibits a marked H depletion in a broad region around the  $R_p$  (marked in Fig. 1b). Although the global H amount, as reported in Table 1, was in this case higher than in the unimplanted sample, (due probably to different substrate contamination levels), the ii-CN<sub>x</sub> film had less hydrogen than the C-film.

##### 3.1.2. Heated films

In Table 1 we give the N, C, O and H amounts in the annealed C and ii-CN<sub>x</sub> samples, as obtained by NRA and ERD. Each kind of samples lost hydrogen on heating. After annealing at 1073 K, most of hydrogen effused out of the samples (74% and 80% in C and ii-CN<sub>x</sub> films respectively). In the annealed ii-CN<sub>x</sub> films, in addition to H losses, appreciable nitrogen losses are also observed.

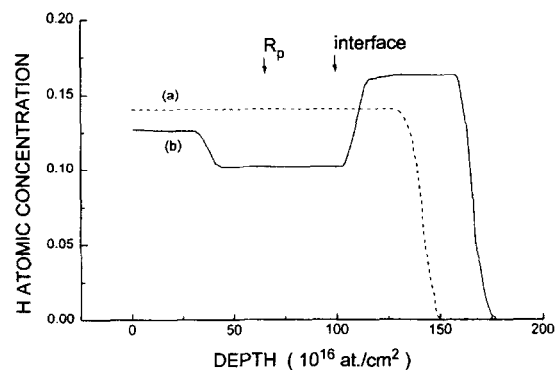


Fig. 1. In-depth hydrogen profiles in C-films (a) before and (b) after  $\text{N}^+$ -implantation.

After annealing at 1073 K, the N amounts are reduced to traces.

### 3.2. N effects on the lattice structure of the carbon films

Raman spectroscopy is a common tool for the characterization of the structure of C-based materials.

Fig. 2a–c compares the Raman spectra of (a) C-film (880 nm thick), (b) an ii-CN<sub>x</sub> film (400 nm thick and implanted with 90 keV N<sup>+</sup>-ions) and (c) a rs-CN<sub>x</sub> film (840 nm thick). The spectrum of the C-film consists of a twin-peaked band. The peaks, broad and almost of equal intensity, develop at about 1360 cm<sup>-1</sup> and 1590 cm<sup>-1</sup>. These bands further broaden and coalesce into a featureless spectrum extending from 1100 cm<sup>-1</sup> to 1800 cm<sup>-1</sup> in the ii-CN<sub>x</sub> spectrum (Fig. 2b). The rs-CN<sub>x</sub> spectrum (Fig. 2c) exhibits the same gross features as the C-film spectrum. The two broad bands observed in the C and the rs-CN<sub>x</sub> film spectra are known to appear in the Raman spectrum of microcrystalline graphite, with cluster size less than 25 nm. The low frequency line is called “D” line and the high frequency one is called “G” line, and they are known to significantly broaden in disordered graphite spectra [12]. The same nomenclature will be used in the following to describe these features in Raman spectra of our films.

Through a fitting procedure of the experimental spectra, more insight into the microstructure of these films can be gained. The three experimental spectra were fitted by three gaussians centered at ~1360 cm<sup>-1</sup> (peak D), ~1500 cm<sup>-1</sup> (peak A) and ~1590 cm<sup>-1</sup> (peak G). The peak at ~1500 cm<sup>-1</sup> is attributed to C–C vibration into an amorphous network, composed of an atomically mixed structure of three- and fourfold-coordinated carbon [13,14]. The additional very sharp line, at 1554 cm<sup>-1</sup>, which appears in each spectra, is related to the presence of O<sub>2</sub> in the films. From these results, the C-films appear as having a composite structure constituted by disordered microcrystalline graphitic domains dispersed in an amorphous matrix, itself formed by sp<sup>2</sup> and sp<sup>3</sup> sites. In order to check the changes brought about by nitrogen to this composite microstructure, we compare the area ratio of the amorphous phase peak to the graphite peak, A/G. The G line was chosen instead of the D line because of its lower sensibility to disorder with respect to the D line [15].

Table 3 gives the A/G ratios for all of the as-prepared and the annealed C-film and both kinds of CN<sub>x</sub> films, as a measure of the degree of amorphicity of the network, along with the D/G ratio as a measure of the disorder of the graphitic phase. The N-incorporation into the C-films appears to increase the amorphicity of the network as it is evidenced by the higher value of the A/G ratio, in the rs- and ii-CN<sub>x</sub> films spectra. The D/G ratio is invariant in the rs-CN<sub>x</sub> film with respect to the C-film, while nitrogen incorporation by ion-implantation resulted in more disordered graphitic domains as shown by the increase of the D/G value [15].

### 3.3. Lattice microstructure evolution of the C and CN<sub>x</sub> films under annealing

Fig. 3a–c shows the Raman spectra from the C-films, the ii-CN<sub>x</sub> film and the rs-CN<sub>x</sub> film respectively, annealed at 1073 K. In these spectra, the A/G values are to

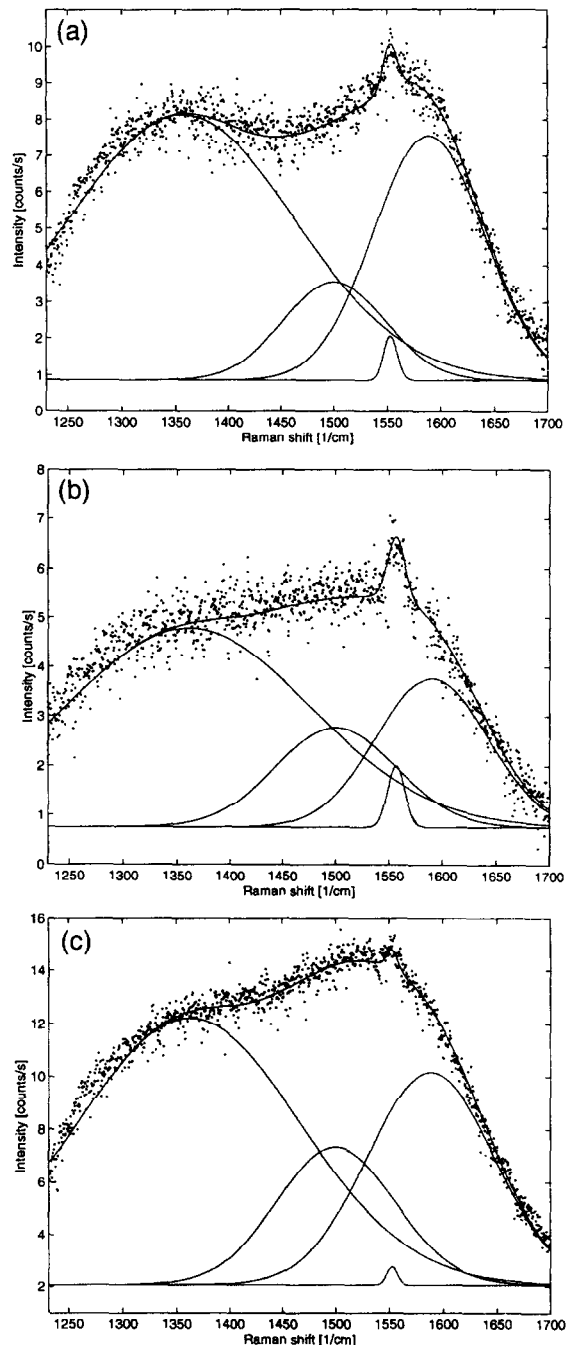


Fig. 2. Raman spectra of as-deposited (a) C-film, (b) ii-CN<sub>x</sub> film and (c) rs-CN<sub>x</sub> film.

compare with those of Fig. 2. Similar to Fig. 2, a fit procedure of the experimental spectra provides a semi-quantitative comparison of the microstructural changes undergone by the C and both kinds of the  $CN_x$  films under annealing. The values of the A/G ratio and the D/G ratio, as obtained from the fitting parameters, are displayed in Table 3, along with those obtained for the same films annealed at 773 K. It comes that heating the C-films at 1073 K resulted in more resolved D and G bands in the spectra (compare Fig. 3a and Fig. 2a) along with a slight decrease of the peak A. The composite structure of the C-films are only slightly affected by annealing, even at 1073 K. The amorphous phase contribution after annealing at 1073 K annealed film dropped by only 20% of its initial value. On the other hand, annealing induced more disorder in the graphitic phase, as shown by the increased D/G values, in contrast to the rs- $CN_x$  films, which gain relatively more homogeneity after annealing. Among the analysed films, both the as prepared and the annealed ii- $CN_x$  films present the highest level of disorder.

The relatively high stability of the C films against graphitization is considerably reduced in the ii- $CN_x$  and rs- $CN_x$  films. Here, again, the experimental spectra of annealed ii- and rs- $CN_x$ , resulted in much more resolved D and G bands, due to a significantly reduced contribution of peak A. After annealing at 1073 K, the A/G ratio value drops to 44% of its initial value in ii- $CN_x$  and the spectrum grossly resembles that of the as-deposited C-film. The same behaviour was observed in the rs- $CN_x$  film, for which the A/G ratio value, after annealing at 1073 K, falls to 36% of its initial value (Table 3). So, both kinds of  $CN_x$  films exhibit a neat tendency to graphitise, in contrast to C-films which retained 80% of their amorphicity after annealing at 1073 K. It is also worthwhile to note that in both rs- and ii- $CN_x$  the graphitisation took place mostly after 773 K, as it can be understood from the variations of the A/G ratios after the 773 K and the 1073 K annealings.

Interestingly, after the 773 K annealing, both  $CN_x$  films and C film graphitise at the same (limited) rate (the A/G ratio is reduced by only 13–15% (Table 3). These results suggest that, at this temperature, the released nitrogen from the ii- $CN_x$  film corresponds primarily to non-bonded or weakly bonded nitrogen species. On the contrary, the pronounced structural changes observed in the ii- $CN_x$  film annealed at 1073 K can be due to the release of chemically bonded nitrogen [5]. Besides, the Raman results indicate that the presence of H does not seem to be critical for the amorphicity of the C-films, may be due to its relatively low concentration and/or to a peculiar lattice structure of the C-films, different from that of hydrogenated films [16]. On the contrary, our results point towards a crucial role of N in stabilising the amorphous component of the carbon network.

#### 3.4. Defect microstructure of the as-prepared and the annealed C and $CN_x$ films

Positron Annihilation Spectroscopy (PAS) is a powerful technique for measuring open volume or vacancy-like defect profiles in near surface regions. The shape of the positron annihilation line, sensible to the momentum distribution of electrons, was characterized by the so called  $S$  parameter. The  $S$  parameter is the ratio of the counts in a central region of the annihilation line and the total counts in the line. Every material is characterised by a proper  $S$  value. The  $S$  parameter increases if positron trapping defects, like open volume or vacancies, are present in the material. As a consequence the curve of the  $S$  parameter as a function of depth can be related to the depth distribution of defect [17].

In Fig. 4 we present the PAS measurements ( $S$  parameter versus depth) on the rs- $CN_x$  film (840 nm thick), C-film (880 nm), and ii- $CN_x$  film (400 nm, implanted with

Table 3

Area ratio D/G between the disordered graphite Raman peaks (D and G) and area ratio G/A between the Raman peak G of the disordered graphite and the peak A of the amorphous phase, before and after annealing at  $T_a = 773$  K and  $T_a = 1073$  K. (Values given in parenthesis are the relative variations of A/G on annealing.)

	Films					
	C		ii- $CN_x$		rs- $CN_x$	
	Before annealing					
A/G	0.37		0.73		0.61	
D/G	2.23		2.95		2.22	
	After annealing					
	$T_a$		$T_a$		$T_a$	
	773 K	1073 K	773 K	1073 K	773 K	1073 K
A/G	0.32	0.29	0.62	0.32	0.52	0.22
(Relative change)	(-13%)	(-20%)	(-15%)	(-56%)	(-15%)	(-64%)
D/G	2.35	2.48	3.3	3.0	2.16	2.06

90 keV energy). In Fig. 5 the modification due to thermal treatment on rs-CN<sub>x</sub> film is shown. All the measurements were normalized to the bulk *S* value of silicon. The mean positron penetration depth,  $\bar{z}$  (in nm) was calculated through the following expression:  $\bar{z} = (A/\rho)E^n$ , where *E* in keV is the positron implantation energy,  $\rho$  is the

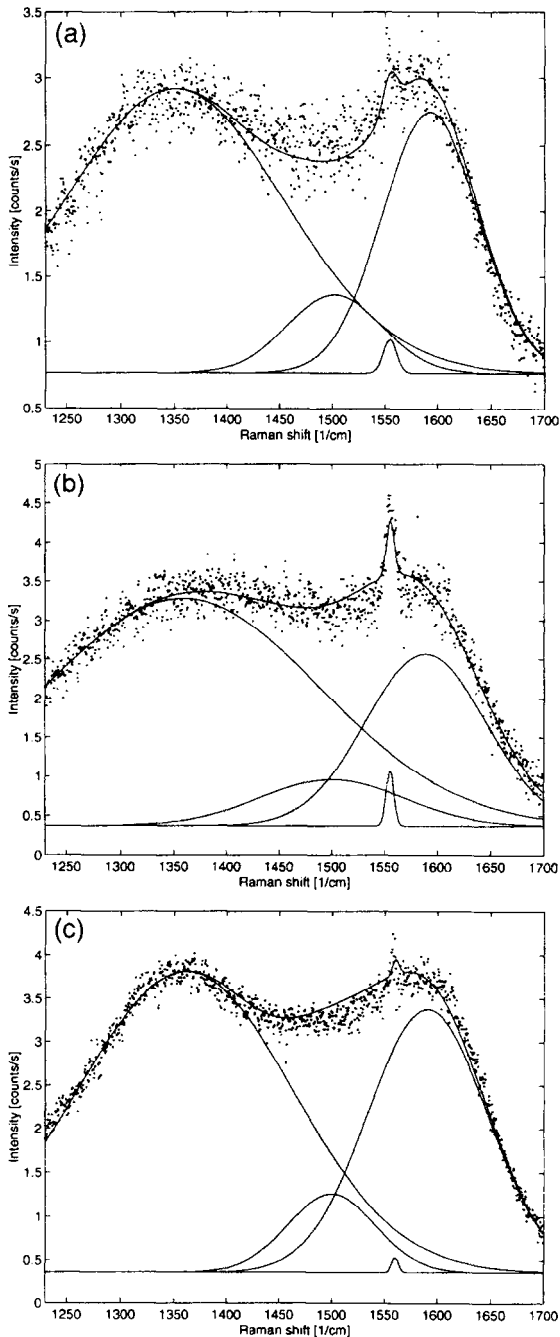


Fig. 3. Raman spectra of (a) C-film, (b) ii-CN<sub>x</sub> film and (c) rs-CN<sub>x</sub> film, annealed at 1073 K.

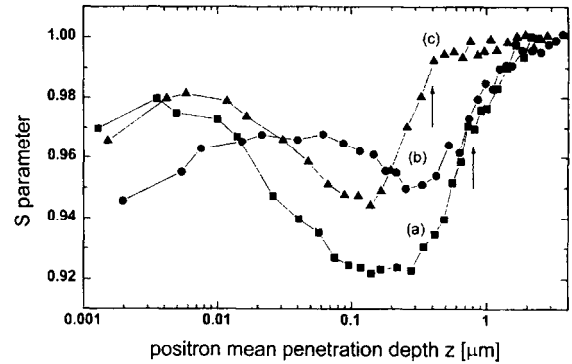


Fig. 4. *S* parameter versus positron mean implantation depth in: (a) rs-CN<sub>x</sub> film, (b) C-film and (c) ii-CN<sub>x</sub> film.

material density in g/cm<sup>3</sup> and  $A = 0.35 \mu\text{g cm}^{-2} \text{keV}^{-n}$ ,  $n = 1.55$  [18]. We took as density values of rs-CN<sub>x</sub>, C-, and ii-CN<sub>x</sub> films those reported in Table 2. The interface film-silicon is arrowed in the figures.

The *S* parameter for the rs-CN<sub>x</sub>, shown in Fig. 4a starts from an almost constant surface *S* value (from 1–10 nm), than decreases and reaches a constant value throughout the film. Finally *S* increases through the interface to reach the bulk *S* value of silicon. The constant value of *S* in the films means that it is homogeneous with a uniform distribution of open volume defects. The *S* parameter of the C-film as a function of mean positron penetration depth (Fig. 4b) is similar in shape to that of rs-CN<sub>x</sub> film. But the absolute *S* value of the homogeneous part is higher, showing that the C-film contains more open-volume defects. Moreover in the C-film, the voids distribution is homogeneous from about 80–90 nm. The first 80–90 nm of this film appear to be more defected. Finally, N<sup>+</sup>-implantation in the C-film (pay attention in Fig. 4c to the different thickness of the film) unexpectedly produce a slightly lower defect concentration than in the starting C-film. In fact one would expect a vacancy-like defects

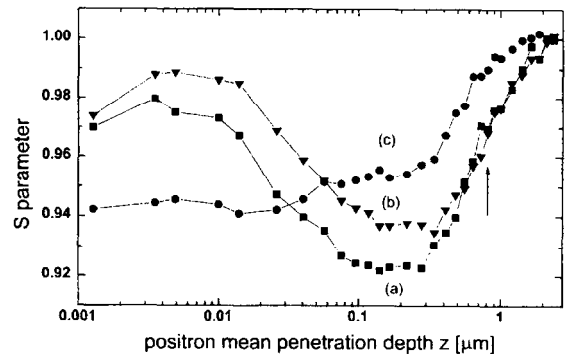


Fig. 5. *S* parameter versus positron mean implantation depth in the rs-CN<sub>x</sub> films: (a) as-deposited, (b) annealed at 773 K and (c) annealed at 1073 K.

distribution due to the implantation process, superimposed to the existing voids distribution. Nevertheless, Raman spectroscopy has shown (Table 3) that in *rs*-CN<sub>x</sub> and *ii*-CN<sub>x</sub> films (films with incorporated nitrogen) the amorphous phase increase with respect to the C-film, and that the graphitic phase is more disordered. So the change in the defect concentration seems to be due to a structural change of the carbon film. In particular the defects probed by positrons seems to be mainly connected to the graphitic disordered phase. In the *ii*-CN<sub>x</sub> the role of injected nitrogen, besides that of partially changing the structure, could be that of refilling the voids.

This interpretation is also supported by the analysis by PAS of the *rs*-CN<sub>x</sub> films annealed at 773 K and 1073 K (Fig. 5). In the sample annealed at 773 K, the *S* parameter curve (curve b) has the same shape than in the as-deposited film (curve a) but is higher in absolute value, indicating an increase in the defect concentration. In the sample annealed at 1073 K, the defect concentration increases again from 30 nm to the interface (curve c). In these samples Raman spectroscopy confirms a continuous graphitization as a function of the annealing temperature (see Table 3) reaching the as-deposited C-film structure at 1073 K. The phenomenon is also assisted by an out diffusion of nitrogen as observed in *ii*-CN<sub>x</sub> annealed samples. Decreasing the defects while rising the nitrogen dose was also recently observed in a-C hydrogenated films [19].

In summary, the analysed films present a uniform distribution of open volume defects. The void concentration in the *ii*-CN<sub>x</sub> and *rs*-CN<sub>x</sub> was lower than in the C-films. In the N-containing films, it increased on annealing, with the degree of graphitization of the material.

#### 4. Conclusion

We have studied the effects of the N incorporation by reactive sputtering and by ion-implantation in C-films on (i) the composite microstructure of these films and (ii) their thermal behaviour. Nitrogen increased the amorphicity of the network whatever be the nitrogenation process and reduced, as well, the void density in the C-films. After annealing at 1073 K, while the amorphicity of the C-films was relatively preserved, in both CN<sub>x</sub> films it was significantly reduced, giving rise to higher amounts of disordered graphitic phase. This process appears to be assisted by the nitrogen effusion out of the films, and it resulted in an increased void density. However, annealings at 773 K did

not result in great changes in the composite microstructure of all of the C-films and the CN<sub>x</sub> films.

#### Acknowledgements

M. Adami, M. Bonelli and E. Voltolini are gratefully acknowledged for the ion implantations.

#### References

- [1] H. Sjöström, I. Ivanov, M. Johansson, L. Hultman and J.-E. Sundgren, *Thin Solid Films* 246 (1994) 103.
- [2] P. Wood, T. Wydeven and O. Tsuji, *Thin Solid Films* 258 (1995) 151.
- [3] K.J. Boyd, D. Marton, S.S. Todorov, A.H. Al-bayati, J. Kulik, R.A. Zuhr and J.B. Rabalais, *J. Vac. Sci. Technol. A* 13 (1995) 2110.
- [4] H. Xin, W. Xu, X. Shi, H. Zhu, C. Lin and S. Zou, *Appl. Phys. Lett.* 66 (1995) 3290.
- [5] N. Laidani, A. Miotello and J. Perriere, *Appl. Surf. Sci.* 99 (1996) 273.
- [6] N. Laidani, A. Miotello, A. Glisenti, C. Bottani and J. Perriere, *J. Phys.: Condens. Matter.*, in press.
- [7] J.F. Ziegler, in: *Handbook of Ion Implantation Technology*, ed. J.F. Ziegler (Elsevier, Amsterdam, 1992) pp. 1–68.
- [8] G. Vizkelethy, *Nucl. Instr. and Meth.* 45 (1990) 1.
- [9] F.W. Smith, *J. Appl. Phys.* 55 (1984) 7664.
- [10] N. Savvides, *J. Appl. Phys.* 59 (1986) 4233.
- [11] J.G. Angus and C.C. Hayman, *Science* 241 (1988) 913.
- [12] H. Tsai and D.B. Bogy, *J. Vac. Sci. Technol. A* 5 (1987) 3287.
- [13] M. Yoshikawa, G. Katagiri, H. Ishida and A. Ishitani, *Solid State Commun.* 66 (1988) 1177.
- [14] R.J. Nemanich, J.T. Glass, G. Lucowsky and R.E. Shroder, *J. Vac. Sci. Technol. A* 6 (1988) 1783.
- [15] M. Shayegan, M.S. Dresselhaus, H. Mazurek and G. Dresselhaus, *Phys. Rev. B* 24 (1981) 1027.
- [16] G. Galli, R.M. Martin, R. Car and M. Parinello, *Phys. Rev. Lett.* 62 (1989) 555.
- [17] R.S. Brusa, M. Duarte Naia, A. Zecca, C. Nobili, G. Ottaviani, R. Tonini and A. Dupasquier, *Phys. Rev. B* 49 (1994) 7271.
- [18] V.S. Ghosh, K.G. Lynn and D.O. Welch, in: *Positron Spectroscopy of Solid — Int. School of Physics Enrico Fermi*, eds. A. Dupasquier and A.P. Mills jr. (IOS Press, Amsterdam, 1995) pp. 683–727.
- [19] F.L. Freire Jr., D.F. Franceschini, R.S. Brusa, G.P. Karwasz, G. Mariotto, A. Zecca and C.A. Achete, *J. Appl. Phys.*, submitted for publication.